Available online at www.sciencedirect.com
SCIENCE DIRECT
Talanta 69 (2006) 829–834
Talanta
www.elsevier.com/locate/talanta

Electroanalytical applications of boron-doped diamond microelectrode arrays

Nathan S. Lawrence [a,*], Markus Pagels [a], Andrew Meredith [a], Timothy G.J. Jones [a], Clive E. Hall [b], C.S. Jim Pickles [b], Herman P. Godfried [b], Craig E. Banks [c], Richard G. Compton [c], Li Jiang [a,**]

[a] *Schlumberger Cambridge Research, High Cross, Madingley Road, Cambridge CB3 0EL, UK*
[b] *Element Six B.V., Beversestraat 20, 5431 SH Cuijk, The Netherlands*
[c] *Physical and Theoretical Chemistry Laboratory, University of Oxford, South Parks Road, Oxford OX1 3QZ, UK*

Received 28 July 2005; received in revised form 25 October 2005; accepted 4 November 2005
Available online 9 December 2005

Abstract

The electrochemical characteristics of a novel all diamond fabricated boron-doped diamond microelectrode array (BDD-MEA) are critically appraised. The voltammetric response of simple electron transfer processes has been investigated and found to generate sigmoidal voltammetric curves. Furthermore, the device has been utilized for various analytical applications including, the direct detection of 4-nitrophenol over the concentration range 1.8–9.2 μM, manganese over the range 0.1–4.8 μM and the indirect determination of sulfide producing a limit of detection of 23 μM.

Keywords: Boron-doped diamond; Microelectrode array; Electrochemistry; Steady state; Analysis

1. Introduction

The use of boron-doped diamond (BDD) as an electrode substrate is now well established due to its four main properties: a wide potential window in aqueous solutions [1], low background currents [2], long term stability [3] and low sensitivity to dissolved oxygen [4,5]. The culmination of these properties makes BDD particularly suited for electrochemical studies of analytes with high oxidation potentials [6]. This has been demonstrated with the plethora of literature now available in which BDD has been used successfully for the detection of a wide range of species (for example: amines [6,7], cysteine [8–10], chlorophenols [11,12], sulfide [13] and other sulfur containing species [14]).

BDD disc electrodes can be fabricated in both macroelectrode ($d > 50\,\mu m$) or microelectrode ($d < 50\,\mu m$) forms. The design of the microelectrode is such that it has significant advantages over conventional macroelectrodes. These include: (a) enhanced mass transport, due to the small diffusion layer across the surface and the convergent diffusion at its edges, allowing steady state limiting currents to be achieved; (b) increased current densities; and (c) decreases in both ohmic drop and charging currents. Although there are numerous advantages to the use of single microelectrodes, there are also disadvantages that might restrict or inhibit their use in field sensing. To overcome these problems, assemblies of microelectrodes have been designed [15–17]. In these systems, the microelectrodes are placed electrically in parallel to each other and such that at suitable scan rates, their diffusional fields do not overlap, i.e. they behave as independent microelectrodes. However, as all the electrodes are connected to a single electrical contact, the signal generated is greatly enhanced when compared to a single microelectrode. It can be foreseen that coupling the advantages of these microelectrode arrays with the usefulness of BDD would produce a powerful electrode device.

To date, four BDD-microelectrode arrays have been reported [18–21]. Fujishima and coworkers [18] device was fabricated by using a photo resist pattern onto which the BDD film was deposited. After this, the surface was spin coated with a polyimide film, which is then mechanically etched producing a

* Corresponding author. Tel.: +44 1223 325224.
** Co-corresponding author.
E-mail address: nlawrenc@cambridge.oilfield.slb.com (N.S. Lawrence).

0039-9140/$ – see front matter © 2005 Elsevier B.V. All rights reserved.
doi:10.1016/j.talanta.2005.11.020

protruding boron-doped diamond array consisting of 200 BDD disks with diameters between 25 and 30 μm and separated by a distance of 250 μm. Rychen and coworkers [19] BDD-array was fabricated by forming a BDD film onto which a silicon nitride layer (5 μm thick) was patterned, resulting in a recessed BDD-MEA. The device consisted of an hexagonal array of 106 BDD disc's, which were 5 μm in diameter, separated by 150 μm. Swain and coworkers [20] have reported on diamond *ultra*microelectrode arrays, based on forming a pattern via photolithography onto a silicon wafer with CVD diamond grown into the mold. These BDD electrodes again are effectively recessed squares. Finally, Madore et al. have reported on BDD-MEA fabricated using CVD deposition and photolithographic techniques producing microdisk electrodes, which were 5 μm in diameter and separated by 100 μm [21]. Recently, we have reported on an all diamond electrode, which consists of individual boron-doped diamond discs, which can have diameters of between 10 and 25 μm, separated from the nearest neighbor by 10 times the disc's diameter [22]. This BDD-array is advantageous since the resulting electrode has no seals or recesses or elevations in contrast to those already reported. The array is in a hexagonal pattern which has been micro-machined to prepare and coat a patterned boron-doped diamond (BDD) substrate with an intrinsic diamond insulating layer and has the advantage of the array being co-planar to the dielectric surroundings. These devices are planar and made entirely of diamond removing the problem of 'sealing' the microelectrodes in their insulating material as experienced with the earlier devices [18–21].

2. Experimental

2.1. Reagents

All reagents were obtained from Aldrich and were of the highest grade available and used without further purification. All aqueous solutions and subsequent dilutions were prepared using deionised water from an Elgastat (Elga, UK) UHQ grade water system with a resistivity of 18 MΩ cm. All other solutions and subsequent dilutions were prepared using acetonitrile (99.9% grade, dried and distilled, Aldrich) usually in 0.1 M tetrabutylammonium perchlorate (TBAP, Fluka).

Stock sulfide solutions (0.05 M) were prepared by dissolving the sodium salt in previously degassed water and were used within 1 h of preparation to minimise losses due to aerial oxidation. All experiments were typically conducted at 20 ± 2 °C.

2.2. Electrochemical apparatus

Electrochemical measurements were recorded using an Autolab PGSTAT 30 computer controlled potentiostat (Eco-Chemie, Netherlands) with a standard three electrode configuration. A platinum wire provided the counter electrode and either a saturated calomel reference electrode (SCE, $Hg/HgCl_2$, Radiometer, Copenhagen) or a silver wire acted as the quasi reference electrode. Either highly polished boron-doped diamond (BDD, 0.031 cm^2, Element Six Ltd., Ascot) or the BDD-MEA served as the working electrode. All the BDD electrodes were housed in a PEEK™ mounting using epoxy (KOFORD, E-109) and consisted of a polished electrode surface that had undergone no pre-treatment.

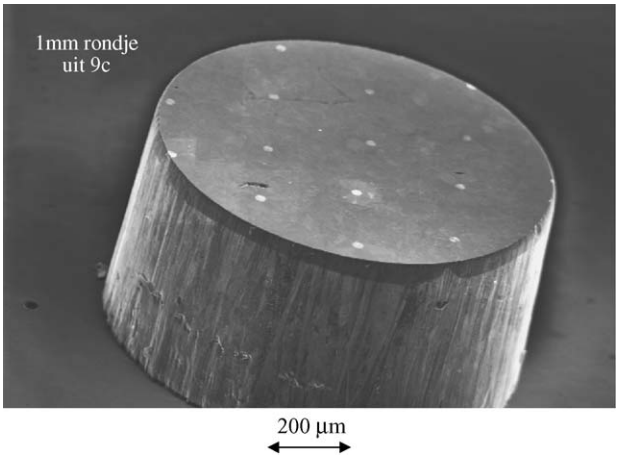

Fig. 1. SEM image of the BDD-MEA (magnification is 1200×).

The voltammetric curves for the manganese data were baseline corrected using Autolab software, which utilises a third-order polynomial correction [23].

2.3. BDD-MEA fabrication

Fig. 1 details a scanning electron microscope (SEM) image of a section (showing 14 electrodes) of the BDD-MEA. In this case, the image was taken at 4 kV in order to prevent the charging of the non-conducting diamond. A full description of the fabrication process is detailed elsewhere [22].

3. Results and discussion

3.1. Electrochemical detection in solutions of low ionic strength

The ability of microelectrodes to deliver steady state responses at suitable scan rates, low analyte concentrations and in the absence of any supporting electrolyte is an attractive feature when comparing them to conventional macroelectrodes [24–27]. These responses are usually obtained when the scan rate is kept low so as to minimize the ohmic drop [28–30]. There are several reasons for conducting both analytical and fundamental studies in the absence of any supporting electrolyte. These include the possibility of conducting analysis directly in samples of low ionic strength, thereby making the analysis more facile, extending the potential window in organic solvents, eliminating the possible interference of the supporting electrolyte in synthetic reactions and providing the possibility of extending the upper concentration limit of the analyte under investigation.

The approximately steady state responses obtained at the BDD-MEA in the absence of any supporting electrolyte and low analyte concentrations are demonstrated in Fig. 2. This depicts the voltammetric response (scan rate = 10 mV s^{-1}) of (a) the 15 μm BDD-MEA, and (b) the BDD macroelectrode for

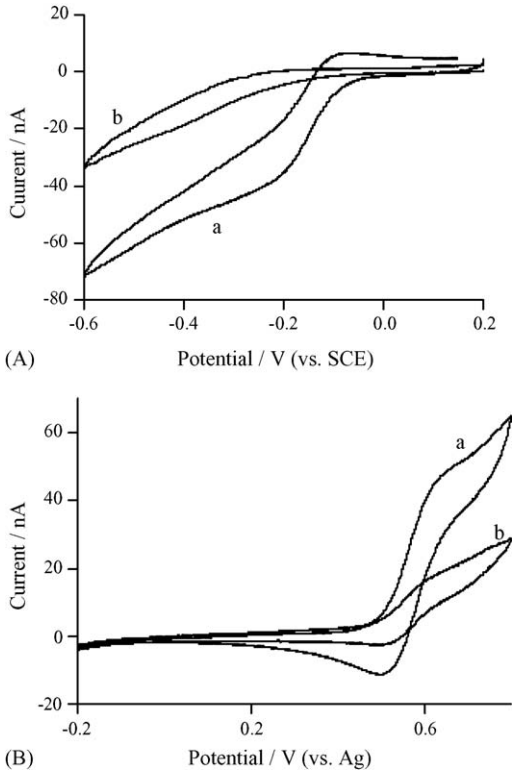

Fig. 2. The cyclic voltammetric responses (scan rate 10 mV s^{-1}) of (a) the 15 μm BDD-MEA and (b) the 1 mm BDD macroelectrode in the presence of (A) 10 μM $Ru(NH_3)_6^{3+}$ in water and (B) 20 μM ferrocene in acetonitrile in the absence of any supported electrolyte.

(A) the reduction of 10 μM $Ru(NH_3)_6^{3+}$ in water, and (B) the oxidation of 20 μM ferrocene in acetonitrile. Analysis of each wave in turn shows that an approximate steady state reduction wave consistent with the one electron reduction of the Ru^{3+} complex is obtained at the BDD-MEA with no defined redox wave obtained at the BDD macroelectrode. It should be noted that the half wave potential (−0.15 V) recorded at the BDD-MEA is consistent with literature values [31]. In contrast, it was found that the ferrocene response produced well-defined redox waves, with half potentials of +0.54 V [32] at both the BDD-MEA and BDD macroelectrodes with the BDD-MEA producing a higher current output. Closer inspection of the curves for both the reduction of the Ru^{3+} complex and the oxidation of ferrocene reveals gentle peaks rather than steady state currents, which indicates a significant contribution to mass transport from planar diffusion, caused by overlapping diffusion zones, i.e. the microdiscs are not diffusionally independent of each other [33]. Moreover, it has been shown via numerical simulations based on the diffusion domain approximation that diffusion overlapping at microelectrode arrays is dependant on the scan rate used and diffusion coefficient [34]. In order to calculate the number of active microelectrodes the following approximation was utilised:

$$I_{\text{lim}} = 4nFDrCN$$

where n is the number of electrons, F is the Faraday constant, r is the radius of the electrode, C is the concentration of the solution and N is the number of active microelectrodes [33]. Using this approximation revealed that there are 150 active microelectrodes on the electrode surface. These results thereby demonstrate the possibility of using the BDD-MEA in solutions without the need for the addition of supporting electrolytes.

3.2. Direct electrochemical detection

We next examined the efficiency of the BDD-MEA for the direct detection of 4-nitrophenol (4-NP). The detection of 4-NP in aqueous media is of great importance as its presence is related to several organophosphorous pesticides (e.g., methyl-parathion, ethyl-parathion, fenitrothion, etc.) and these decompose in water and soils with 4-NP being produced as an intermediate or final product [35,36]. The US Environmental Protection Agency have set the allowed limit of 4-NP in waste waters at 0.22 μM [37]. The determination of 4-NP has been conducted at hanging mercury drop [38], bismuth coated [39] and boron-doped diamond [40] electrodes, with the analytical signal being derived from the 4-electron reduction of the nitro moiety.

Fig. 3a details the reductive linear sweep response (scan rate = 100 mV s^{-1}) at the bare BDD-MEA both in the absence and in the presence of increasing additions of 1.8 μM 4-NP (pH

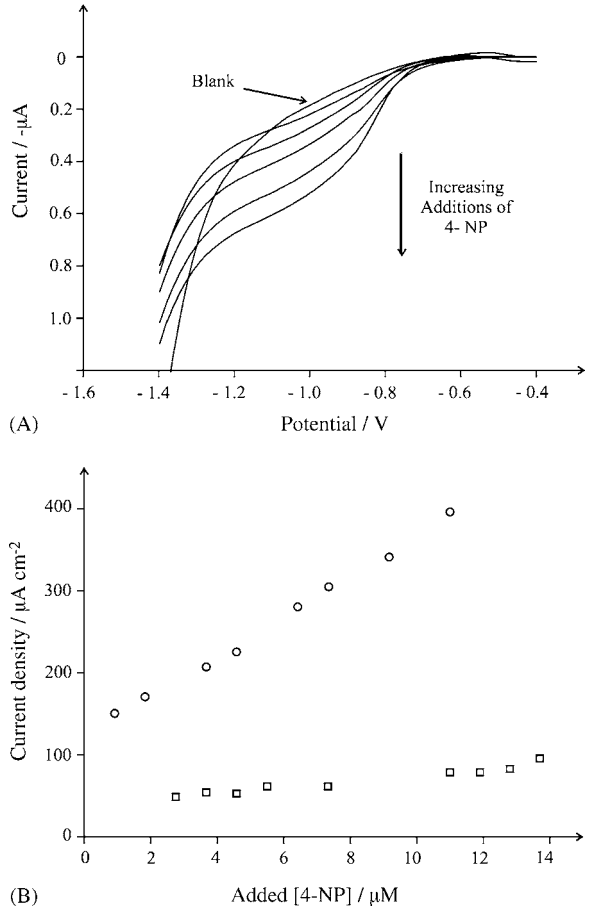

Fig. 3. (A) Linear sweep voltammograms (100 mV s^{-1}) detailing the response obtained at the BDD-MEA in the presence of additions of 4-nitrophenol (4-NP). Actual concentrations are 1.8, 3.7, 5.5, 7.3 and 9.2 μM. (B) A plot of current density as a function of the 4-NP concentration obtained at both the BDD macroelectrode (squares) and BDD-MEA (circles).

6.8, phosphate buffer solution). Upon the addition of 4-NP to the solution, approximately sigmoidal shaped curves are observed at −1.1 V. These waveshapes are consistent with those detailed in Fig. 2A and B. The occurrence of this wave is due to the electrochemical reduction of 4-NP directly at the BDD-MEA, to first form nitrosophenol then further to aminophenol, upon increasing additions the limiting current continues to enhance over the concentration range studied 1.8–9.2 μM.

A plot of the variation in current density measured at both the BDD-MEA and BDD macro electrodes as a function of the 4-NP concentration is displayed in Fig. 3b. This shows that the BDD-MEA shows a ca. seven-fold increase in the sensitivity when compared to the macro electrode and hence serves to demonstrate the analytical utility of the BDD-MEA over the BDD macro electrode. Note here that the non-zero intercepts in the calibration plots can be attributed to uncorrected background charging currents.

3.3. Electrochemical determination of manganese

Manganese is an essential nutrient of the human body and plays a significant role in cellular metabolism at the trace level [41]. It is known, for example, that tea contains a high level of manganese (as high as 1800 μg/g) with 30% of the content in tea known to be in the form of manganese(II). Although manganese is an essential micronutrient for plants and animals, it is also toxic at high levels; chronic manganese poisoning affects the central nervous systems and can contribute to neurological disease [42]. The maximum allowed concentration of manganese in domestic water supplies is 0.05 $\mu g\,L^{-1}$ while the concentrations in excess of 1 $mg\,g^{-1}$ in the diet are required before signs of toxicity are observed [43].

The cathodic stripping voltammetry (CSV) of manganese is a favoured analytical protocol due to its specificity. The technique is based on first applying a pre-concentration step, where, employing a suitable electrode substrate, the electrode potential is held sufficiently positive to form insoluble manganese(IV) dioxide on the electrode surface:

$$Mn^{2+} - 2e + 2H_2O \rightarrow MnO_2 + 4H^+$$

After a chosen pre-concentration time, the potential is then swept negative producing a characteristic voltammetric stripping peak arising from the reduction of manganese(IV) dioxide back to manganese(II) [23].

The response of the BDD-MEA for manganese(II) detection was explored. Using square wave (SW)-CSV with a deposition time of 120 s at +0.85 V (versus SCE), 106 nM aliquots of manganese(II) were added to a 0.5 M ammonium nitrate buffer (pH 7.5) solution. The solution composition, deposition time and potential were chosen based on literature reports, which allows the direct comparison of the present results with existing techniques [44].

Fig. 4 shows the voltammetric responses from the manganese additions with a well-defined stripping peak corresponding to the reduction of manganese dioxide to manganese(II) observed at +ca. 0.43 V which is in good agreement with previous studies [23,44].

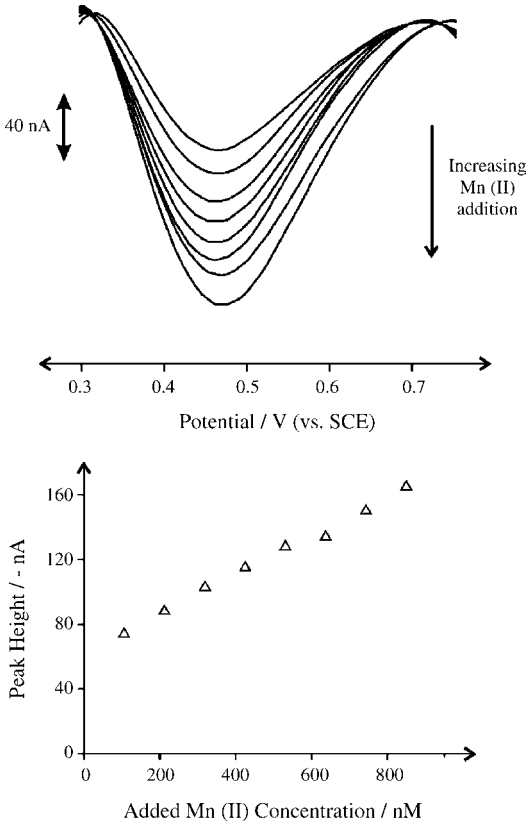

Fig. 4. Square wave-cathodic stripping voltammograms for the addition of increasing 106 nM manganese(II) aliquots into a 0.5 M ammonium nitrate solution (pH 7.5) using the BDD-array. Experimental parameters: 120 s deposition at +0.85 V (vs. SCE); frequency 102 Hz; step potential 8 mV; amplitude 79 mV. Also shown is the corresponding plot of peak current vs. added manganese concentration.

The analysis of the peak height (I_H) versus added manganese concentration was found to produce a linear response over the range 106–849 nM ($I_H/A = 0.118\,([Mn^{2+}]/M) + 6.32 \times 10^{-8}$; $R^2 = 0.998$). Based on 3 sigma, the limit of detection is found to correspond to 49 nM which is an order of magnitude lower than that observed by Goodwin et al., using a macro BDD electrode with identical deposition time/potential and solution composition [44]. Further note that if we compare the sensitivity in terms of active area with that of Goodwin et al., we find their sensitivity to correspond to 34.4 $A\,M^{-1}\,cm^{-2}$ whilst for the BDD-array, this is 71.9 $A\,M^{-1}\,cm^{-2}$ (based on the active area) which is ca. two times higher.

Note that beyond the observed linear range in this study, further additions were found to be unresponsive with the stripping peak becoming irreproducible. The electrode was taken out and polished and placed back into the solution. This produced a large voltammetric response, approximately double the peak height of the last addition on the calibration plot. It is well-documented that incomplete stripping can occur [45] on BDD electrodes. We infer that as additions of manganese are made and the calibration curve constructed, manganese dioxide is built up on the individual microdiscs due to incomplete stripping such that at the end of the observed calibration plot (see Fig. 4), further additions of manganese are deposited onto un-stripped manganese diox-

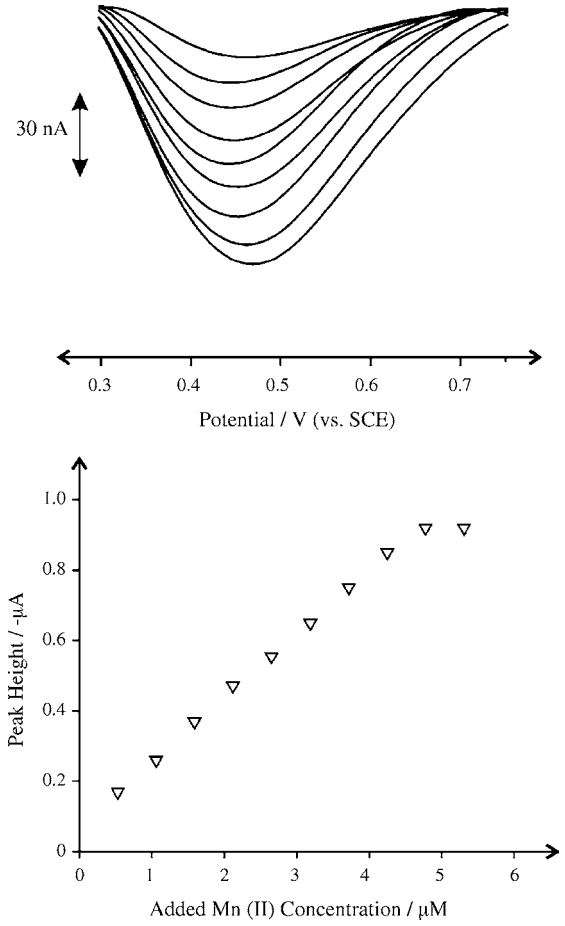

Fig. 5. Square wave-cathodic stripping voltammograms arising from the addition of 530 nM additions of manganese(II) to a 0.5 M ammonium nitrate buffer (pH 7.5). Deposition time is 60 s, all other experimental conditions as in Fig. 4.

ide rather than bare BDD leading to poor reproducibility and a limited linear range.

To extend the linear range into the micromolar region, the deposition time was decreased to 60 s to allow less manganese to build up on the electrode surface. Five hundred and thirty nanomitre additions of manganese(II) were added to a 0.5 M ammonium nitrate solution (pH 7.5) using the BDD-array. Analysis of the resulting peak height versus added manganese concentration was found to produce a linear response from 0.53 to 4.78 μM: linear regression: $I_H/A = 0.179$ ($[Mn^{2+}]/M) + 7.9 \times 10^{-8}$; $R^2 = 0.9988$). (A limit of detection was found to be 0.3 μM.)

Again note that the BDD-array did not respond to further additions. This is shown in Fig. 5 where the next addition results in a 'plateau'. This indeed limits the linear range, which again is attributed to manganese building up on the individual microelectrodes due to incomplete stripping. However, the linear range is sufficient for analytical purposes at the trace level.

3.4. Detection via an electrochemically initiated reaction

A third application of the MEA is their use in electrochemical gas sensing cells, such as for hydrogen sulfide. One detection route for this toxic gas (and its related compounds), studied

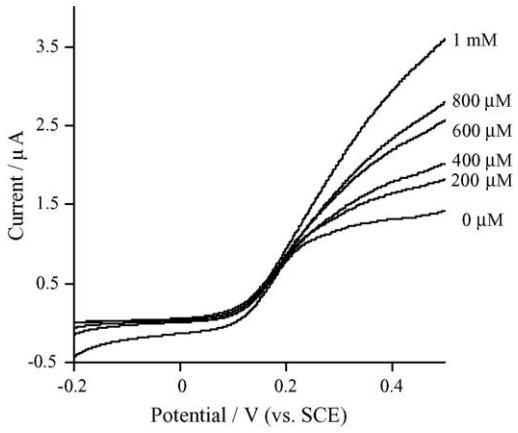

Fig. 6. Linear sweep voltammograms (scan rate = 10 mV s^{-1}) detailing the response of ferrocyanide (1 mM, 0.05 M KH_2PO_4 and 0.05 K_2HPO_4, pH 7) to increasing aliquots of sulfide (200 μM) at the 15 μm BDD-MEA.

at both platinum and BDD electrodes is their electrocatalytic reaction with ferrocyanide [46,47]. If the catalytic reaction is sufficiently fast, so as to occur within the diffusion layer of the microelectrode [48], then the BDD-MEA could be used in a hydrogen sulfide sensor.

Fig. 6 illustrates the linear sweep voltammetric response of ferrocyanide (1 mM, pH 7 phosphate buffer, scan rate = 10 mV s^{-1}) at the 15 μm BDD-MEA electrode. A steady state oxidation wave is observed at +0.25 V (versus SCE). Also depicted in Fig. 6 is the change in the voltammetric response when multiple additions of 200 μM sulfide are introduced to the ferrocyanide solution. Upon the introduction of sulfide, an increase in the oxidative limiting current is observed. This is consistent with the ferrocyanide being oxidised to ferricyanide directly at the electrode surface. In the presence of sulfide, the newly generated ferricyanide is immediately reduced back to ferrocyanide, which is reoxidised at the electrode surface thus producing the catalytic enhancement in the oxidative wave [47]. Analysis of the standard addition plot (not shown) yielded a limit of detection of 23 μM (based on $3s_b$).

4. Conclusion

The electrodes have shown to be of analytical use, first with the steady state behaviour observed in media with no supporting electrolyte, proffering the possibility of analysis directly in environmental samples and thereby obviating the need for supporting electrolyte. Secondly, the enhanced sensitivity of the BDD-MEA over the conventional macro electrode has been demonstrated in the detection of 4-NP, a result which could have significant implication for environmental sampling.

Furthermore, the electrode has been successfully utilised with anodic stripping voltammetry for the determination of manganese. The results show a significant advantage in utilizing these electrodes over a conventional planar macroelectrode. Finally, it has been demonstrated that electrochemically initiated reactions can occur at the electrode surface. This will allow the arrays to be used in detection processes, which rely upon this type of reaction chemistry for detection to take place and

also offers the possibility of the BDD-MEA to be utilized in thin layer gas sensor cells.

This new BDD-MEA electrode design offers some advantages over the existing two BDD-MEA currently available. As the surface is entirely diamond, the electrode will be extremely hard and therefore should be able to be deployed in harsh conditions where more fragile electrodes may break down.

References

[1] J.W. Strojek, M.C. Granger, T. Dallas, M.W. Holtz, G.M. Swain, Anal. Chem. 68 (1996) 2031.
[2] T. Yano, D.A. Tryk, K. Hashimoto, A. Fujishima, J. Electrochem. Soc. 145 (1998) 1870.
[3] E. Popa, H. Notsu, T. Miwa, D.A. Tryk, A. Fujishima, Electrochem. Solid State Lett. 2 (1999) 49.
[4] T.N. Rao, I. Yagi, T. Miwa, D.A. Tryk, A. Fujishima, Anal. Chem. 71 (1999) 2506.
[5] T. Yano, E. Popa, D.A. Tryk, K. Hashimoto, A. Fujishima, J. Electrochem. Soc. 146 (1999) 1081.
[6] R.G. Compton, J.S. Foord, F. Marken, Electroanalysis 15 (2003) 1349.
[7] A. Fujishima, T.N. Rao, E. Popa, V.B. Sarada, I. Yagi, D.A. Tryk, J. Electroanal. Chem. 173 (1999) 179.
[8] T.N. Rao, V.B. Sarada, D.A. Tryk, A. Fujishima, J. Electroanal. Chem. 491 (2000) 175.
[9] O. Chailapakul, E. Popa, H. Tai, V.B. Sarada, D.A. Tryk, A. Fujishima, Electrochem. Commun. 2 (2000) 422.
[10] N. Spataru, V.B. Sarada, E. Popa, D.A. Tryk, A. Fujishima, Anal. Chem. 73 (2001) 514.
[11] A.J. Saterlay, J.S. Foord, R.G. Compton, Electroanalysis 13 (2001) 1065.
[12] C. Prado, G. Murcott, R.G. Compton, Electroanalysis 14 (2002) 975.
[13] J.A. Reynaud, B. Maltoy, P.J. Canessan, J. Electroanal. Chem. 114 (1980) 195.
[14] O. Chailapakul, P. Aksharanandana, T. Freilink, Y. Einaga, A. Fujushima, Sens. Actuators B 80 (2001) 193.
[15] R.L. Deutscher, S. Fletcher, J. Electroanal Chem. 239 (1998) 17.
[16] S. Fletcher, in: M.I. Montengro, M.A. Queiros, J.L. Dashbach (Eds.), Microelectrodes: Theory and Applications, Kluwer, Dordrecht, 1991, p. 341.
[17] S. Fletcher, M.D. Horne, Electrochem. Commun. 1 (1999) 502.
[18] K. Tsunozaki, Y. Einaga, T.N. Rao, A. Fujishima, Chem. Letts. 5 (2002) 502.
[19] C. Provent, W. Haenni, E. Santoli, P. Rychen, Electrochim. Acta 49 (2004) 3737.
[20] K.L. Soh, W.P. Kang, J.L. Davidson, S. Basu, Y.M. Wong, D.E. Cliffel, A.B. Bonds, G.M. Swain, Diamond Relat. Mater. 13 (2004) 2009.
[21] C. Madore, A. Duret, W. Haenni, A. Perret, Proc. Electrochem. Soc., 2000-19 (Microfabricated Systems and MEMS V), (2000) 159.
[22] M. Pagels, C.E. Hall, N.S. Lawrence, A. Meredith, T.G.J. Jones, H.P. Godfried, C.S.J. Pickles, J. Wilman, C.E. Banks, R.G. Compton, L. Jiang, Anal. Chem. 77 (2005) 3705.
[23] A.J. Saterlay, J.S. Foord, R.G. Compton, Analyst 124 (1999) 1791.
[24] A.M. Bond, M. Fleischmann, J. Robinson, J. Electroanal. Chem. 168 (1984) 299.
[25] A.M. Bond, M. Fleischmann, J. Robinson, J. Electroanal. Chem. 172 (1984) 11.
[26] A.G. Ewing, B.J. Feldman, R.W. Murray, J. Phys. Chem. 89 (1985) 1263.
[27] R.M. Wightman, Science 240 (1988) 415.
[28] K.B. Oldham, J. Electroanal. Chem. 237 (1987) 303.
[29] S. Bruckenstein, Anal. Chem. 59 (1987) 2098.
[30] A.M. Bond, D. Luscombe, K.B. Oldham, C.G. Zoski, J. Electroanal. Chem. 249 (1988) 1.
[31] M.J. Moorcroft, N.S. Lawrence, B.A. Coles, L.N. Triviani, R.G. Compton, J. Electroanal. Chem. 506 (2001) 28.
[32] B.A. Coles, M.J. Moorcroft, R.G. Compton, J. Electroanal. Chem. 513 (2001) 87.
[33] A.O. Simm, C.E. Banks, S. Ward-Jones, T.J. Davies, N.S. Lawrence, T.G.J. Jones, L. Jiang, R.G. Compton, Analyst 130 (2005) 1303.
[34] T.J. Davies, S. Ward-Jones, C.E. Banks, J. del Campo, R. Mas, F.X. Muñoz, R.G. Compton, J. Electroanal. Chem. 585 (2005) 51.
[35] M. Castillo, R. Domingues, M.F. Alpendurada, D. Barcelo, Anal. Chim. Acta 353 (1997) 133.
[36] S.V. Dzyadevych, J.M. Chovelon, Mater. Sci. Eng. C 21 (2002) 55.
[37] S. Environmental Agency, Fer. Regist. 44 (1979) 233.
[38] J. Barek, H. Ebertova, V. Mejstrik, J. Zima, Collect. Czech Chem. C 59 (1994) 1761.
[39] E.A. Hutton, B. Ogorevc, M.R. Smyth, Electroanalysis 16 (2004) 1616.
[40] V.A. Pedrosa, L. Codognoto, S.A.S. Machado, L.A. Avaca, J. Electroanal. Chem. 573 (2004) 11.
[41] A.R. McEuen, Inorganic Biochemistry, Royal Society of Chemistry, London, 1981.
[42] A. Iregren, Neurotoxicology 15 (1994) 671.
[43] E.J. Underwood (Ed.), Trace Elements in Human and Animal Nutrition, Academic Press, New York, 1997.
[44] A. Goodwin, A.L. Lawrence, C.E. Banks, F. Wantz, D. Omanovic, E. Komorsky-Lovric, R.G. Compton, Anal. Chim. Acta 533 (2005) 141.
[45] M.E. Hyde, C.E. Banks, R.G. Compton, Electroanalysis 16 (2004) 345.
[46] P. Jeroschewski, K. Haase, A. Trommer, P. Gründler, Fres. J. Anal. Chem. 346 (1993) 930.
[47] N.S. Lawrence, M. Thompson, C. Prado, L. Jiang, T.G.J. Jones, R.G. Compton, Electroanalysis 14 (2002) 499.
[48] B. Brookes, N.S. Lawrence, R.G. Compton, J. Phys. Chem. B 104 (2000) 11258.